

000 001 002 003 004 005 006 007 008 009 010 011 012 013 014 015 016 017 018 019 020 021 022 023 024 025 026 027 028 029 030 031 032 033 034 035 036 037 038 039 040 041 042 043 044 045 046 047 048 049 050 051 052 053 GUI-SHIFT: ENHANCING VLM-BASED GUI AGENTS THROUGH SELF-SUPERVISED REINFORCEMENT LEARN- ING

006
007 **Anonymous authors**
008 Paper under double-blind review

010 011 ABSTRACT

013 Training effective Vision-Language Models (VLMs) for GUI agents typically
014 depends on large-scale annotated datasets, whose collection is both labor-intensive
015 and error-prone. We introduce ***K*-step GUI Transition**, a self-supervised inverse
016 dynamics task in which VLMs learn GUI dynamics by predicting the initial action
017 that causes a transition between two GUI states. This approach eliminates the
018 need for natural language instructions and enables scalable dataset construction
019 from existing GUI trajectories or automated exploration. Building on this task, we
020 propose **GUI-Shift**, a reinforcement learning (RL) framework that combines rule-
021 based optimization with data filtering to improve VLM performance. We conduct
022 extensive experiments using multiple VLM backbones across four benchmarks,
023 spanning GUI task automation (AndroidControl, GUI Odyssey) and GUI grounding
024 (ScreenSpot-v2, ScreenSpot-Pro). Our results show that training on GUI-Shift
025 generalizes well to both GUI automation and grounding tasks, yielding up to an
026 11.2% increase in GUI automation accuracy. This study underscores the potential
027 of self-supervised RL to leverage unlabeled GUI trajectories and offers a scalable
028 alternative to training with annotated samples.

029 030 1 INTRODUCTION

031 Mobile GUI agents (Gou et al., 2024; Hong et al., 2024; Qin et al., 2025; Wen et al., 2024; Yang
032 et al., 2024) interpret natural language instructions and perform actions (e.g., click, scroll) directly
033 on smartphone screens. They can control diverse apps as a human would, improving accessibility
034 for users who are visually impaired, elderly, or have their hands occupied. Breakthroughs of vision
035 language models (VLMs) (Bai et al., 2025; Chen et al., 2024; Xiaomi, 2025b) have reshaped the
036 design paradigm of mobile GUI agents, transitioning from handcrafted heuristics to learned, vision-
037 grounded policies. However, VLMs still struggle to deliver satisfactory accuracy (Dai et al., 2025;
038 Qin et al., 2025; Rawles et al., 2024; Zhang et al., 2025a), especially when facing complex multi-
039 step tasks. A common approach for enhancing VLMs is through supervised fine-tuning (SFT) on
040 datasets containing GUI interaction trajectories paired with human-annotated task instructions (Li
041 et al., 2024; Rawles et al., 2023). Yet effective, collecting GUI trajectories with task instructions
042 remains labor-intensive and error-prone (Deka et al., 2017; Rawles et al., 2023). For example, the
043 AndroidControl (Li et al., 2024) dataset takes one year of paid annotation effort to produce just
15,283 task demonstrations. Such high annotation cost limits the scalability of this paradigm.

044 In this study, we aim to address a fundamental challenge: *how to train capable mobile GUI agents*
045 *using large-scale, unlabeled GUI trajectories, rather than relying on costly human-annotated in-*
046 *structions*. To tackle this, we propose a self-supervised training task, termed ***K*-step GUI Transition**.
047 Inspired by inverse-dynamics modeling in robotics and biomechanics (Brandfonbrener et al., 2023;
048 Tian et al., 2024; Zapsolsky & Drumwright, 2017), where a model predicts control commands linking
049 two consecutive physical states, our task treats screenshots as states and GUI actions as commands.
050 Each training sample in *K*-step GUI Transition consists of two screenshots, S_t and S_{t+k} , where
051 S_{t+k} results from executing k actions starting from S_t . The VLM is trained to predict the first action
052 that transforms S_t into S_{t+1} . This design offers two key advantages: (1) *Explicit state-change signal*.
053 Each sample contains a pair of GUI screenshots, enabling the model to utilize inter-screen visual
differences and temporal cues, rather than learning from a single screen. (2) *Efficient data utilization*

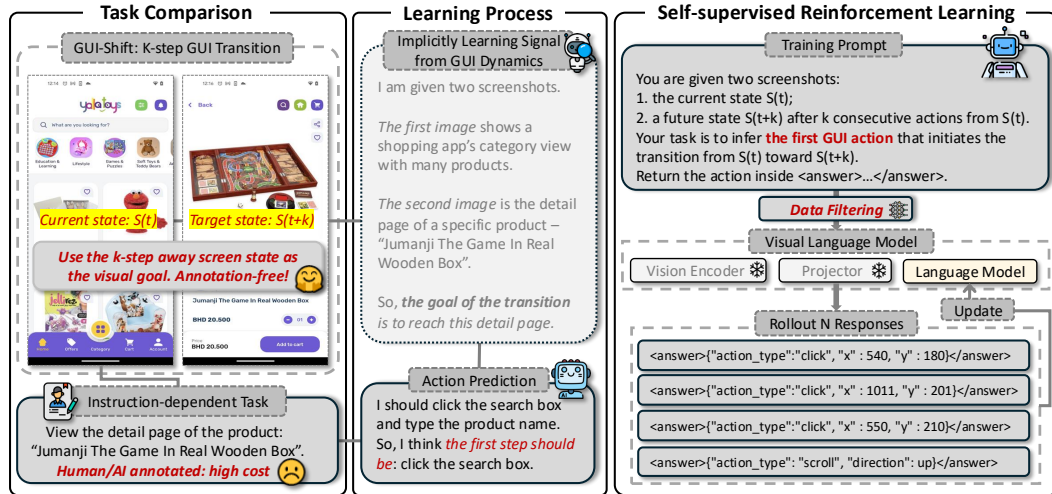


Figure 1: **Overview of the GUI-Shift framework.** **Left:** *K*-step GUI Transition replaces annotated instructions with the target state S_{t+k} , enabling scalable data construction through automated offline exploration. **Middle:** The model learns GUI dynamics by predicting the action that causes the transition. **Right:** GUI-Shift achieves self-supervised training by applying GRPO to GUI Transition.

at scale. Since ground-truth actions are embedded in GUI trajectories (Rawles et al., 2023; Li et al., 2024), no predefined instructions or manual annotations are needed. Moreover, for any k , a GUI trajectory with n screens can yield up to $n - k$ training samples, enabling scalable data construction. These benefits make *K*-step GUI Transition a strong candidate for self-supervised GUI agent training.

With the self-supervised training task, it is essential to determine how to effectively enhance VLMs. In GUI tasks, multiple action parameters can often be functionally equivalent and result in the same next state. For example, any coordinate within a button’s bounding box is valid for a click, and textual inputs may be accepted in various formats or with different keywords. This multiplicity makes supervised fine-tuning (SFT) suboptimal, as it enforces a single reference action in a static dataset through the cross-entropy loss, penalizing all other valid alternatives and therefore providing misleading learning signals. To address this limitation, we adopt Group Relative Policy Optimization (GRPO) (Shao et al., 2024), which samples diverse plausible actions, evaluates them using a task-specific reward function, and ranks them based on group-normalized advantages. For example, in click actions, rewards are assigned if the sampled point lies within the target bounding box, offering a more tolerant and informative optimization signal. Overall, GRPO provides a more effective training paradigm for GUI agents by encouraging exploration and increasing robustness to action variability.

To this end, we present GUI-Shift, a self-supervised reinforcement learning (RL) framework that applies GRPO to *K*-step GUI Transition. Figure 1 illustrates the overview of the GUI-Shift framework. To select data matched to the model’s learning ability, we adopt a unified action sampling and scoring mechanism during both data filtering and training stages. For each sample, the VLM generates N action predictions, each scored based on format and action correctness. Only samples containing both correct and incorrect predictions among the N predictions are selected for training. After training, the VLM acquires GUI-specific capabilities and serves as a more effective backbone for GUI agents. VLMs enhanced with GUI-Shift also have the ability to generalize well to GUI task automation and GUI grounding tasks without further alignment or fine-tuning.

We apply GUI-Shift to train four VLMs: Qwen2.5-VL-7B (Bai et al., 2025), InternVL3-8B (Chen et al., 2024), MimoVL-7B-SFT (Xiaomi, 2025b), and MimoVL-7B-RL, each using 2K samples for four *K*-step GUI Transition variants ($k \in \{1, 2, 3, 4\}$). We evaluate the VLMs on four benchmarks: AndroidControl (Li et al., 2024) and GUI Odyssey (Lu et al., 2024) for GUI task automation, and ScreenSpot-v2 (Wu et al., 2024b) and ScreenSpot-Pro (Li et al., 2025a) for GUI grounding. Overall, VLMs enhanced with GUI-Shift show notable improvements over their base versions. For example, GUI-Shift-Qwen achieves up to 11.2% higher accuracy on AndroidControl-High and 2.5% on ScreenSpot-v2, yielding 70.4% and 89.0% overall accuracy on the respective benchmarks. We also

108 conduct comprehensive ablation studies to examine the effects of data filtering, task formulation,
 109 reasoning configurations, and training paradigms. The results show that using the target state S_{t+k} as
 110 a visual instruction offers an effective alternative to human- or AI-annotated textual instructions for
 111 training GUI agents. The key contributions are summarized below.
 112

113 (1) We introduce K -step GUI Transition, a training task that leverages abundant unlabeled GUI
 114 trajectories to enhance VLMs used in GUI agents.
 115

116 (2) We propose GUI-Shift, a self-supervised RL framework that bridges the gap between GUI
 117 dynamics modeling and action-level GUI learning, mitigating the limitation of SFT in
 118 handling action multiplicity and poor generalization in GUI tasks.
 119

120 (3) Experiments across four VLMs and four benchmarks show that VLMs enhanced with GUI-
 121 Shift exhibit generalization in both GUI automation and grounding tasks, with up to 11.2%
 122 accuracy gains.
 123

124 2 RELATED WORK

125 2.1 MOBILE GUI AGENTS

126 Recent progress in mobile GUI agents has been driven by VLMs trained via SFT on large-scale
 127 datasets. These models learn to map instructions to GUI actions using instruction-following tasks,
 128 making high-quality annotations essential. Despite the availability of diverse GUI datasets (Deka et al.,
 129 2017; Gao et al., 2024; Li et al., 2024; Lu et al., 2024; Rawles et al., 2023), the quantity of high-quality
 130 annotations remains insufficient for robust training and usually requires significant human effort to
 131 scale. To reduce annotation costs, prior pipelines often incorporate out-of-domain image-caption
 132 pairs (Hong et al., 2024; Wang et al., 2024) and supplement training with web and desktop data to
 133 improve cross-platform generalization (Cheng et al., 2024). As a result, the overall scale of training
 134 data tends to be large: Uground (Gou et al., 2024) uses 1.3M screenshots to train a visual grounding
 135 model; OS-Atlas (Wu et al., 2024b) leverages 13M GUI elements for grounding pretraining. Some
 136 recent approaches have explored GUI state modeling. UI-TARS (Qin et al., 2025) incorporates a state
 137 transition task, which focuses on describing visual changes between screenshots rather than predicting
 138 the underlying actions, resulting in a gap with GUI task automation. MobileVLM (Wu et al., 2024a)
 139 introduces an action prediction task between screenshots, but is restricted to one-step transitions and
 140 SFT. They still rely on annotation-heavy fine-tuning for downstream alignment and generalization. In
 141 this work, we propose K -step GUI Transition, formulating a k -step inverse dynamics objective that
 142 enables scalable training on large, unlabeled, and underutilized GUI datasets.
 143

144 2.2 RULE-BASED REINFORCEMENT LEARNING

145 Rule-based RL has proven to be a promising alternative to SFT. GRPO (Shao et al., 2024) uses a re-
 146 ward model to score each response and computes group relative advantages instead of training a critic
 147 model, whose size is comparable to the policy model, thereby significantly reducing computational
 148 cost. Reinforcement Learning with Verifiable Rewards (Lambert et al., 2024) further emphasize the
 149 use of verifiable answers to design reliable reward signals. DeepSeek-R1 (Guo et al., 2025) shows
 150 that simple format and accuracy rewards are sufficient to surpass the performance of instruction-tuned
 151 models. Several recent works have applied GRPO on GUI tasks: UI-R1 (Lu et al., 2025) employs
 152 one-stage RL on 136 samples with step-level instructions. GUI-R1 (Xia & Luo, 2025) expands this
 153 to 3K task-level instructions from five platforms. InfiGUI-R1 (Liu et al., 2025) adopts a two stage
 154 SFT+RL pipeline and scales to 32K samples from both GUI and non-GUI domains. UI-Venus (Gu
 155 et al., 2025) employs GRPO to two variants, using 107K samples for grounding and 350K for naviga-
 156 tion. While these works demonstrate the effectiveness of rule-based RL for GUI agents, they still rely
 157 on annotated instructions and require reasoning during training and inference. Different from these
 158 annotation-dependent training paradigms, GUI-Shift fine-tunes VLMs via one-stage RL on K -step
 159 GUI Transition in a self-supervised manner, achieving competitive performance and demonstrating
 160 strong generalization across GUI task automation and GUI grounding benchmarks.
 161

162

3 METHODOLOGY

163

164 GUI-Shift is a self-supervised RL framework designed to enhance VLM-based GUI agents through
165 the K -step GUI Transition task. In this section, we first describe GRPO, the underlying training
166 algorithm in GUI-Shift. We then detail the reward design tailored to GUI action modeling, and
167 present the complete GUI-Shift framework along with its rationale and advantages.

168

3.1 PRELIMINARIES

169

170 GRPO (Shao et al., 2024) offers a computationally efficient alternative to Proximal Policy Optimization (PPO) (Schulman et al., 2017), a widely used actor-critic method. Instead of maintaining a
171 separate critic network for value estimation, GRPO computes normalized, group-wise advantages A_i
172 directly from reward scores, thereby removing the value function update and lowering computational
173 cost. The GRPO objective in our framework is defined as follows:

174
$$\begin{aligned} \mathcal{J}_{\text{GRPO}}(\theta) &= \mathbb{E} \left[q \sim P(Q), \{o_i\}_{i=1}^G \sim \pi_{\theta_{\text{old}}}(O \mid q) \right] \\ &\quad \frac{1}{G} \sum_{i=1}^G \left(\min(\rho_i A_i, \text{clip}(\rho_i, 1 - \epsilon, 1 + \epsilon) A_i) - \beta \mathbb{D}_{\text{KL}}(\pi_\theta \parallel \pi_{\text{ref}}) \right), \end{aligned} \quad (1)$$
175
$$\text{where } \rho_i = \frac{\pi_\theta(o_i \mid q)}{\pi_{\theta_{\text{old}}}(o_i \mid q)}, \quad A_i = \frac{r_i - \text{mean}(\{r_1, r_2, \dots, r_G\})}{\text{std}(\{r_1, r_2, \dots, r_G\})}.$$
176

177 Specifically, for each question q in the training set, we sample a group of outputs $\{o_1, o_2, \dots, o_G\}$
178 from the old policy $\pi_{\theta_{\text{old}}}$ using high temperature decoding, and compute the group-wise relative
179 advantage A_i for each output. A clipped surrogate objective, along with a KL divergence regularizer
180 toward the reference policy π_{ref} , is then used to update model parameters and ensure training stability.

181

3.2 REWARD DESIGN

182

183 The reward function plays a central role in guiding and stabilizing model optimization. In GUI action
184 prediction, each answer is a structured action comprising a verifiable action type and associated
185 parameters, making the task well-suited to a rule-based reward formulation. Following DeepSeek-
186 R1 (Guo et al., 2025), we adopt a rule-based reward R tailored for GUI tasks, which combines a format
187 reward R_f to enforce output consistency and an action reward R_a to evaluate action correctness:

188
$$R = R_f + R_a \quad (2)$$
189

190 **Format reward.** To ensure that model outputs are well-structured and easy to parse, GUI-Shift
191 requires the final answer to be enclosed in `<answer>...</answer>` tags during training. Pre-
192 dictions conforming to the expected format receive $R_f = 1$; otherwise, $R_f = 0$. Unlike prior
193 methods (Lu et al., 2025; Liu et al., 2025; Xia & Luo, 2025), GUI-Shift omits explicit reasoning
194 traces in outputs, eliminating reasoning token generation and substantially reduces training time. For
195 example, training Qwen2.5-VL-7B on 2K K -step GUI Transition samples requires only 9 hours,
196 compared to 17 hours with reasoning traces, without compromising downstream performance, as
197 shown in Table 3.

198 **Action reward.** We adopt a unified action space of eight types for both training and inference.
199 The action space comprises eight types, each as a JSON object with `action_type` and type-specific
200 parameters: `click` and `long_press` require a target point; `scroll` requires a direction; `open_app` requires
201 an app name; `input_text` requires the input content; and `navigate_back`, `navigate_home` and `wait`
202 require no parameters. The action reward R_a is defined accordingly:

203
$$R_a = \begin{cases} 1, & \text{if } x_1 \leq \hat{x} \leq x_2 \text{ and } y_1 \leq \hat{y} \leq y_2, \quad t \in \{\text{click}, \text{long_press}\}; \\ 1, & \text{if } \hat{t} = t \text{ and } \hat{p} = p, \quad t \in \{\text{open_app}, \text{input_text}, \text{scroll}\}; \\ 1, & \text{if } \hat{t} = t, \quad t \in \{\text{navigate_back}, \text{navigate_home}, \text{wait}\}; \\ 0, & \text{otherwise.} \end{cases} \quad (3)$$
204

205 Here, \hat{t} and \hat{p} denote the predicted action type and parameter, t and p denote their ground-truth
206 counterparts; \hat{x}, \hat{y} are the predicted coordinates, and $[x_1, y_1, x_2, y_2]$ is the ground-truth bounding box.

216
217

3.3 GUI-SHIFT FRAMEWORK

218
219
220
221
222
223
224
225
226
227
228
229
230

K-step GUI Transition. While existing VLMs can parse individual GUI screens due to exposure to GUI data during pretraining, they still lack the temporal reasoning capabilities required for complex multi-step GUI tasks. To bridge this gap, we propose the K -step GUI Transition task, which asks the model to predict the first action that transitions a given state S_t to a future state S_{t+k} , as shown in Figure 1. Compared to annotated approaches, our task offers two key advantages. First, while annotated tasks require costly and error-prone textual annotations for each step, K -step GUI Transition leverages state pairs directly extracted from GUI trajectories. The future state S_{t+k} , obtained after executing k actions from S_t , serves as an explicit visual goal, providing a supervision signal that is not only annotation-free but also more concrete and informative than textual instructions. Second, rather than mapping textual instructions to actions, our task compels the model to interpret and compare both the current and target GUI states, infer the transition goal, and identify the action that initiates the state change. Overall, by leveraging visual goals and requiring temporal reasoning across state pairs, this more challenging formulation fosters a deeper understanding of GUI dynamics and provides a scalable, practical solution for robust GUI agent training.

231
232
233
234
235
236
237
238
239
240
241

Self-supervised RL. During training, for each sample, the model generates N candidate actions ($N = 8$ in our experiments), each evaluated by a rule-based reward that integrates format and action correctness, as detailed in Section 3.2. Group-wise normalized advantages are then computed, and optimization proceeds as outlined in Section 3.1. GRPO is particularly well-suited to GUI-Shift for three reasons: (1) Compared to PPO, it eliminates the need for a separate value function, typically in the same size as the policy model. This substantially reduces computational overhead and better supports our efficiency objectives; (2) Compared to SFT, it enables flexible reward assignment tailored to each action type. For instance, click actions are considered correct if the predicted point falls within the ground-truth bounding box rather than requiring an exact match in SFT, which better reflects practical GUI grounding requirements; (3) The N -candidate sampling mechanism encourages exploration and model can learn from optimal candidates while avoiding suboptimal ones.

242
243
244
245
246
247
248
249

Data filtering pipeline. To prepare high-quality K -step GUI Transition data, we perform data filtering using the same action sampling and scoring mechanism as in training. First, for each $k \in \{1, 2, 3, 4\}$, we construct a pool of candidate state pairs (S_t, S_{t+k}) from the original dataset. Next, for each pair, the model generates 8 responses using the same sampling temperature as in GRPO training. Each response is then evaluated with the reward function described in Section 3.2. Finally, we retain only those pairs with both correct and incorrect responses. By applying this filtering process to each model independently, the final training set is both challenging and informative, and well aligned with the model’s learning capacity.

250
251
252
253
254
255
256
257

Taken together, these design choices enable GUI-Shift to provide higher efficiency from three aspects: (1) *Scalable data construction.* Without relying on annotated instructions, GUI-Shift enables large-scale filtering of training data at minimal cost. For example, for Mimo-VL-7B-RL, we filtered 2,920 high-quality samples out of 8K original 1-step GUI Transition pairs, without any annotation waste. (2) *Maximized data utilization.* For each k , an n -image trajectory can yield up to $n - k$ training pairs, maximizing data utilization for fixed-length GUI trajectories. (3) *Reduced training cost.* Without explicit reasoning traces during training, GUI-Shift avoids extra token decoding and reduces training time by nearly 50%, from 17 to 9 hours on 2K samples under our experimental setup.

258
259

4 EXPERIMENTS

260
261
262
263
264
265
266

In this section, we first detail the experimental setup, including data construction and training configurations (Section 4.1). We then present results for models trained with K -step GUI Transition ($k \in \{1, 2, 3, 4\}$), emphasizing improvements over base models and comparisons with existing baselines on GUI task automation and grounding benchmarks (Section 4.2). To further verify the design choices in GUI-Shift, we conduct comprehensive ablation studies from four perspectives: data filtering, task formulation, reasoning configurations during RL, and training algorithms (Section 4.3).

267
268
269

4.1 EXPERIMENTAL SETUP

Training configurations. Using the open-source VLM-R1 (Shen et al., 2025) framework, we fine-tune Qwen2.5-VL-7B (Bai et al., 2025), InternVL3-8B (Chen et al., 2024), MimoVL-7B-SFT, and

270 MimoVL-7B-RL (Xiaomi, 2025b) with the pipeline described in Section 3. During training, only the
 271 language model is optimized while the vision encoder and projector are frozen. All experiments are
 272 conducted on 8×NVIDIA H100 GPUs. Hyper-parameters are listed in Appendix B.
 273

274 **Data construction.** All training data are sourced from the training set of AndroidControl (Li et al.,
 275 2024), which provides GUI trajectories paired with human-labeled instructions. These instructions
 276 enable both self-supervised GUI-Shift training and comparisons with VLMs trained using SFT (see
 277 Section 4.3 for a comparison of the two training approaches). Following the data filtering pipeline
 278 discussed in Section 3, we select 2K samples per k for each model. For Qwen2.5-VL-7B, the
 279 proportion of samples with either entirely correct or entirely incorrect actions was exceptionally high.
 280 As a result, we use unfiltered data for its training.
 281

282 4.2 BENCHMARKS AND RESULTS

283 **GUI task automation.** We evaluate GUI-Shift on two task automation benchmarks: *AndroidControl* (Li et al.,
 284 2024) and *GUI Odyssey* (Lu et al., 2024). *AndroidControl* provides two test settings:
 285 *AndroidControl-Low*, which assesses step-level instruction following ability (e.g., “Type the product
 286 name in the search box”), and *AndroidControl-High*, which evaluates long-horizon task planning (e.g.,
 287 “View the detail page of the product”). *GUI Odyssey* offers a more challenging evaluation, encompassing
 288 both phone and tablet applications as well as cross-app scenarios. The test set includes 9,134
 289 samples in *AndroidControl* and 27,493 in *GUI Odyssey*, covering six action types: *click*, *long_press*,
 290 *scroll*, *navigate_back*, *navigate_home*, and *input_text*. We report *type match* (TM) that represents the
 291 proportion of samples with the correct action type, and *exact match* (EM), which requires both the
 292 action type and all parameters to be correct. Metrics are computed using AgentCPM-GUI (Zhang
 293 et al., 2025b) and GUIEvalKit (Xiaomi, 2025a).
 294

295 Table 1: Performance comparison on GUI task automation benchmarks: *AndroidControl* (AC-Low,
 296 AC-High) and *GUI Odyssey*. GUI-Shift achieves substantial improvements over base models. **Bold**:
 297 the best result; underlined: the second best result. TM: type match; EM: exact match.

299 300 Model	# Training 301 Samples	AC-Low		AC-High		GUI Odyssey	
		TM	EM	TM	EM	TM	EM
<i>Proprietary models</i>							
GPT-4o (OpenAI, 2024)	-	74.3	19.4	66.3	20.8	34.3	3.3
<i>Models trained with annotations</i>							
SeeClick (Cheng et al., 2024)	1M	93.0	75.0	82.9	59.1	71.0	53.9
OS-Atlas-7B (Wu et al., 2024b)	2.3M	93.6	85.2	85.2	71.2	-	62.0
Aguvis-7B (Xu et al., 2024)	1M	-	80.5	-	61.5	-	-
UI-TARS-7B (Qin et al., 2025)	-	98.0	90.8	83.7	72.5	94.6	87.0
UI-R1-3B (Lu et al., 2025)	136	94.3	88.5	57.9	45.4	52.2	32.5
GUI-R1-7B (Xia & Luo, 2025)	3K	85.2	66.5	71.6	51.7	65.5	38.8
InfiGUI-R1-3B (Liu et al., 2025)	32K	96.0	92.1	82.7	71.1	-	-
AgentCPM-GUI (Liu et al., 2025)	470K	94.4	90.2	77.7	69.2	<u>90.9</u>	<u>75.0</u>
UI-Venus-Navi-7B (Gu et al., 2025)	350K	97.1	<u>92.4</u>	86.5	76.1	87.3	71.5
<i>Ours: Qwen2.5-VL-7B as the base model</i>							
Qwen2.5-VL-7B (Bai et al., 2025)	-	94.9	83.8	72.9	59.2	59.8	44.9
GUI-Shift-Qwen ($k = 1$)	2K	98.0 <u>↑3.1</u>	90.6 <u>↑6.8</u>	85.9 <u>↑13.0</u>	70.4 <u>↑11.2</u>	78.5 <u>↑18.7</u>	54.8 <u>↑9.9</u>
<i>Ours: InternVL3-8B as the base model</i>							
InternVL3-8B (Chen et al., 2024)	-	97.8	90.0	71.5	49.8	48.8	20.3
GUI-Shift-Intern ($k = 4$)	2K	97.3 <u>↓0.5</u>	88.0 <u>↓2.0</u>	78.5 <u>↑7.0</u>	56.6 <u>↑6.8</u>	59.6 <u>↑10.8</u>	23.3 <u>↑3.0</u>
<i>Ours: Mimo-VL-7B-SFT as the base model</i>							
Mimo-VL-7B-SFT (Xiaomi, 2025b)	-	90.8	85.7	75.2	63.1	86.9	62.0
GUI-Shift-Mimo-SFT ($k = 3$)	2K	<u>98.6</u> <u>↑7.8</u>	93.2 <u>↑7.5</u>	87.2 <u>↑12.0</u>	<u>73.4</u> <u>↑10.3</u>	86.1 <u>↓0.8</u>	60.7 <u>↓1.3</u>
<i>Ours: Mimo-VL-7B-RL as the base model</i>							
Mimo-VL-7B-RL (Xiaomi, 2025b)	-	91.8	87.2	76.5	64.6	87.2	63.1
GUI-Shift-Mimo-RL ($k = 1$)	2K	98.9 <u>↑7.1</u>	93.2 <u>↑6.0</u>	<u>86.9</u> <u>↑10.4</u>	<u>71.7</u> <u>↑7.1</u>	84.8 <u>↓2.4</u>	59.5 <u>↓3.6</u>

• *GUI-Shift generally improves performance over base models on GUI task automation benchmarks.* Table 1 presents the results of GUI-Shift, together with comparisons against both base models and models trained with annotations. GUI-Shift achieves notable gains across all four models, especially on AndroidControl-High. GUI-Shift-Qwen raises EM by 11.2% over Qwen2.5-VL-7B, while GUI-Shift-Mimo-SFT and GUI-Shift-Mimo-RL reach gains of 10.3% and 7.1%, respectively. On GUI Odyssey, minor declines for GUI-Shift-Mimo-SFT and GUI-Shift-Mimo-RL likely result from the 1,381 tablet episodes in the test set, whose GUI layouts differ substantially from smartphones. Compared to models trained with annotations, GUI-Shift achieves comparable or even superior results on all benchmarks using only 2K K -step GUI Transition samples. Overall, these results underscore the robustness and effectiveness of our approach in GUI task automation.

GUI grounding. We evaluate GUI-Shift on two GUI grounding benchmarks: *ScreenSpot-v2* (Wu et al., 2024b) with 1,272 samples from mobile, desktop, and web platforms, and *ScreenSpot-Pro* (Li et al., 2025a) with 1,581 high-resolution screenshots for fine-grained evaluation. Evaluations for the base models and GUI-Shift are adapted from ScreenSpot-Pro-GUI-Grounding (Li et al., 2025b).

• *GUI-Shift consistently outperforms base models and surpasses most existing baselines on GUI grounding benchmarks.* Table 2 summarizes the overall and baseline results. Across all models, GUI-Shift delivers improved accuracy over base models, with the best variants reaching 2.5% and 1.5% gains on ScreenSpot-v2 and ScreenSpot-Pro, respectively. Moreover, GUI-Shift surpasses all annotation-trained models except UI-Venus-Ground-7B, which is trained specifically for the GUI grounding using 107K annotated samples. These results demonstrate that models trained solely on unlabeled GUI Transition data can effectively transfer to challenging GUI grounding tasks.¹

Table 2: Performance comparison on GUI grounding benchmarks: ScreenSpot-v2 and ScreenSpot-Pro. GUI-Shift exhibits strong generalization and achieves the second best result on ScreenSpot-Pro. **Bold:** the best result; underlined: the second best result.

Model	# Training Samples	ScreenSpot-v2						-Pro	
		Mobile		Desktop		Web		Avg.	Avg.
Models trained with annotations									
CogAgent-18B (Wang et al., 2024)	-	-	-	-	-	-	-	-	7.7
SeeClick-9.6B (Cheng et al., 2024)	1M	78.4	50.7	70.1	29.3	55.2	32.5	55.1	1.1
UGround-7B (Gou et al., 2024)	1.3M	75.1	84.5	85.1	61.4	84.6	71.9	76.3	16.5
OS-Atlas-7B (Wu et al., 2024b)	2.3M	95.2	75.8	90.7	63.6	90.6	77.3	84.1	18.9
ShowUI-2B (Lin et al., 2024)	256K	-	-	-	-	-	-	-	7.7
UI-TARS-7B (Qin et al., 2025)	-	96.9	89.1	<u>95.4</u>	85.0	93.6	85.2	<u>91.6</u>	35.7
UI-R1-E-3B (Lu et al., 2025)	2K	83.0	97.1	85.0	91.7	77.9	95.4	89.5	33.5
InfiGUI-R1-3B (Liu et al., 2025)	32K	-	-	-	-	-	-	-	35.7
LPO (Tang et al., 2025)	-	97.9	82.9	95.9	86.4	95.6	84.2	90.5	-
UI-Venus-Ground-7B (Gu et al., 2025)	107K	99.0	<u>90.0</u>	97.0	<u>90.7</u>	96.2	<u>88.7</u>	94.1	50.8
Ours: Qwen2.5-VL-7B as the base model									
Qwen2.5-VL-7B (Bai et al., 2025)	-	98.3	86.3	88.7	67.1	92.7	81.8	87.7	26.4
GUI-Shift-Qwen ($k = 4$)	2K	<u>98.6</u>	89.6	86.1	75.0	92.7	82.8	89.0 $\uparrow 1.3$	27.1 $\uparrow 0.7$
Ours: InternVL3-8B as the base model									
InternVL3-8B (Chen et al., 2024)	-	93.4	81.5	80.4	52.1	91.0	73.4	81.3	15.0
GUI-Shift-Intern ($k = 1$)	2K	93.8	83.4	80.4	51.4	91.0	73.4	81.6 $\uparrow 0.3$	15.4 $\uparrow 0.4$
Ours: Mimo-VL-7B-SFT as the base model									
Mimo-VL-7B-SFT (Xiaomi, 2025b)	-	96.6	84.4	92.8	80.0	88.9	76.8	87.6	39.8
GUI-Shift-Mimo-SFT ($k = 1$)	2K	98.3	87.7	92.3	82.1	94.0	79.8	90.1 $\uparrow 2.5$	40.7 $\uparrow 0.9$
Ours: Mimo-VL-7B-RL as the base model									
Mimo-VL-7B-RL (Xiaomi, 2025b)	-	<u>98.3</u>	86.3	90.2	80.7	92.7	75.4	88.4	40.2
GUI-Shift-Mimo-RL ($k = 1$)	2K	99.0	87.7	91.2	83.6	89.7	72.9	88.4 $\uparrow 0.0$	41.7 $\uparrow 1.5$

¹Detailed results for different k values are provided for GUI task automation and GUI grounding benchmarks in Appendix C and Appendix D, respectively.

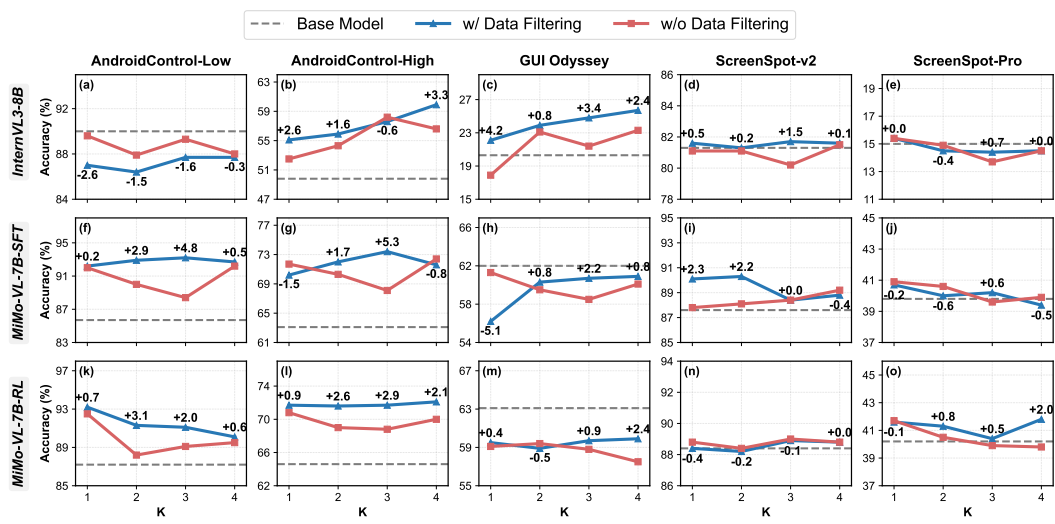


Figure 2: Impact of Data filtering. Each model is fine-tuned on 2K K -step GUI Transition samples. Filtered data are more informative and challenging, and outperform unfiltered ones.

4.3 ABLATION STUDY

Data filtering. We evaluate InternVL3-8B, MimoVL-7B-SFT, and MimoVL-7B-RL trained with and without data filtering on both GUI task automation and GUI grounding benchmarks. For each K -step GUI Transition sample, each model generates 8 responses to build its candidate pool, retaining only those samples where predictions are both correct and incorrect. We select 2K training samples per model and k from each filtered pool and the original training set, respectively.

• *Data filtering improves accuracy on both GUI task automation and GUI grounding benchmarks.* Figure 2 shows that models trained with filtered data achieve higher accuracy than those trained on unfiltered data in most cases. For example, on AndroidControl-Low, MimoVL-7B-SFT achieves up to 4.8% higher accuracy (Figure 2(f), $k=3$), and on ScreenSpot-v2, up to 2.3% (Figure 2(i), $k=1$). These results suggest that our filtering mechanism effectively selects more informative and challenging samples for GUI agent training. Moreover, since K -step GUI Transition does not require human-annotated instructions, this filtering process scales easily and incurs minimal cost.

Task formulation. We compare K -step GUI Transition with two annotated baselines. To ensure fairness, we do not apply data filtering, and all models in each comparison are trained on the same set of 2K samples, with identical current states S_t and ground-truth actions. The only difference is the instruction type: baselines pair S_t with a human-annotated *task instruction* or *step instruction*, while K -step GUI Transition uses the target state S_{t+k} as the visual instruction.

• *Using S_{t+k} as the visual target outperforms using textual instructions as input.* Table 3 shows that VLMs trained with K -step GUI Transition achieves better performance than those with annotated tasks in most cases. For example, on AC-Low and AC-High, InternVL3-8B trained with GUI Transition achieves 4.0% and 3.6% higher EM accuracy, respectively, than when trained with task instructions. Qwen2.5-VL-7B also achieves the highest EM accuracy with GUI Transition across all benchmarks. These results indicate that S_{t+k} provides a more informative signal than human-annotated instructions.

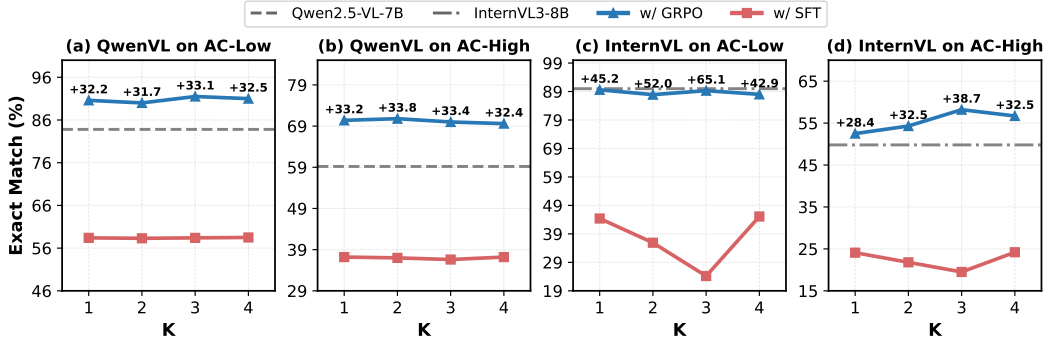
Reasoning configurations. To verify the effect of reasoning during training, we compare models fine-tuned on 2K K -step GUI Transition data with and without `<think>...</think>`.

• *Excluding reasoning boosts performance and efficiency for GUI-Shift.* Table 3 shows that omitting explicit reasoning requirements during training not only maintains but often improves performance. For InternVL3-8B, training without reasoning achieves up to 7.9% higher EM on AndroidControl-High; Qwen2.5-VL-7B shows consistent gains of about 2% across benchmarks. Moreover, removing reasoning nearly halves training time cost, reducing it from 17 to 9 hours for Qwen2.5-VL-7B and

432
 433 Table 3: Performance on GUI task automation under different training settings. GUI-Shift outper-
 434 forms models trained with textual instructions or with explicit reasoning requirements. **Bold**: the best
 435 result. TM: type match; GR: grounding accuracy for clicks; EM: exact match.

436 437 438 Model	439 AndroidControl-Low			440 AndroidControl-High			441 GUI Odyssey		
	442 TM	443 GR	444 EM	445 TM	446 GR	447 EM	448 TM	449 GR	450 EM
<i>Base model: Qwen2.5-VL-7B</i>									
Qwen2.5-VL-7B	94.9	90.9	83.8	72.9	66.6	59.2	59.8	47.5	44.9
+ Task Instruction	97.9 ^{↑3.0}	93.5 ^{↑2.6}	90.5 ^{↑6.7}	85.3 ^{↑12.4}	76.2 ^{↑9.6}	69.9 ^{↑10.7}	74.1 ^{↑14.3}	62.0 ^{↑14.5}	51.8 ^{↑6.9}
+ Step Instruction	97.7 ^{↑2.8}	93.7 ^{↑2.8}	86.4 ^{↑2.6}	82.4 ^{↑9.5}	73.1 ^{↑6.5}	67.2 ^{↑8.0}	74.5 ^{↑14.7}	62.7 ^{↑15.2}	51.5 ^{↑6.6}
<i>Ours (w/ reasoning)</i>	95.5 ^{↑0.6}	91.1 ^{↑0.2}	88.2 ^{↑4.4}	83.8 ^{↑10.9}	75.6 ^{↑9.0}	69.0 ^{↑9.8}	74.0 ^{↑14.2}	63.5 ^{↑16.0}	51.6 ^{↑6.7}
<i>Ours</i>	98.0^{↑3.1}	94.0^{↑3.1}	90.6^{↑6.8}	85.9^{↑13.0}	77.5^{↑10.9}	70.4^{↑11.2}	78.5^{↑18.7}	67.2^{↑19.7}	54.8^{↑9.9}
<i>Base model: InternVL3-8B</i>									
InternVL3-8B	97.8	92.4	90.0	71.5	54.6	49.8	48.8	20.2	20.3
+ Task Instruction	95.9 ^{↓1.9}	92.8^{↑0.4}	85.3 ^{↓4.7}	79.7 ^{↑8.2}	65.8 ^{↑11.2}	54.6 ^{↑4.8}	57.3 ^{↑8.5}	31.5 ^{↑11.3}	26.5 ^{↑6.2}
+ Step Instruction	96.8 ^{↓1.0}	92.8 ^{↑0.4}	86.0 ^{↓4.0}	80.7^{↑9.2}	66.0^{↑11.4}	54.5 ^{↑4.7}	62.6^{↑13.8}	34.4^{↑14.2}	28.8^{↑8.5}
<i>Ours (w/ reasoning)</i>	97.3 ^{↓0.5}	92.3 ^{↑0.1}	87.8 ^{↓2.2}	72.4 ^{↑0.9}	55.8 ^{↑1.2}	50.3 ^{↑0.5}	38.9 ^{↓9.9}	18.8 ^{↓1.4}	16.2 ^{↓4.1}
<i>Ours</i>	97.5^{↓0.3}	92.6 ^{↑0.2}	89.3^{↓0.7}	78.6 ^{↑7.1}	61.7 ^{↑7.1}	58.2^{↑8.4}	51.4 ^{↑2.6}	21.4 ^{↑1.2}	21.4 ^{↑1.1}

451 from 15 to 7 hours for InternVL3-8B. These results confirm that excluding reasoning both improves
 452 performance and significantly enhances training efficiency.



465 Figure 3: Comparison of training algorithms for the K -step GUI Transition task ($k \in \{1, 2, 3, 4\}$).
 466 Qwen2.5-VL-7B and InternVL3-8B are fine-tuned with 2K samples for each k and evaluated on
 467 AndroidControl. GRPO provides notable performance gains over SFT for all models and settings.
 468

469 **Training algorithms.** For each $k \in \{1, 2, 3, 4\}$, we fine-tune Qwen2.5-VL-7B and InternVL3-8B on
 470 2K identical K -step GUI Transition data using SFT or GRPO, and evaluate them on AndroidControl.

471 • *GRPO is more suitable than SFT for K -step GUI Transition.* Figure 3 shows that GRPO improves
 472 accuracy in most cases, whereas SFT consistently reduces accuracy compared to both the base models
 473 and GRPO, with drops up to 65.1% relative to GRPO (Figure 3(c), $k = 3$). We attribute this to its
 474 sensitivity to format mismatch between training and evaluation. These results confirm that GRPO is a
 475 more effective choice for transferring K -step GUI Transition knowledge to GUI task automation.

477 5 CONCLUSION

479 This study introduces GUI-Shift, a self-supervised reinforcement learning framework for training
 480 VLM-based GUI agents without relying on costly annotations. Based on the K -step GUI Transition
 481 training task, enhancing VLMs with GUI-Shift captures temporal dynamics between GUI states
 482 and provides a scalable, annotation-free training signal. Experiments across four VLMs and four
 483 benchmarks show consistent improvements, including up to 11.2% gains in GUI task automation
 484 accuracy and strong generalization to GUI grounding tasks. These results demonstrate that self-
 485 supervised RL can effectively exploit unlabeled GUI trajectories, offering a practical and efficient
 486 alternative to training tasks with human-annotated instructions.

486 ETHICS STATEMENT
487488 This work exclusively uses publicly available, open-source datasets and VLMs, without private or
489 sensitive information. All data sources and models are properly cited and comply with their respective
490 licenses. We have adhered to the ICLR Code of Ethics and are not aware of any ethical concerns
491 regarding this submission.
492493 REPRODUCIBILITY STATEMENT
494495 We have provided detailed descriptions of data construction, model architecture, and experimental
496 settings in the main paper and Appendix. All code and datasets necessary for reproducing our results
497 will be released upon acceptance to ensure full reproducibility.
498499 REFERENCES
500501 Shuai Bai, Keqin Chen, Xuejing Liu, Jialin Wang, Wenbin Ge, Sibo Song, Kai Dang, Peng Wang,
502 Shijie Wang, Jun Tang, et al. Qwen2. 5-vl technical report. *arXiv preprint arXiv:2502.13923*,
503 2025.504 David Brandfonbrener, Ofir Nachum, and Joan Bruna. Inverse dynamics pretraining learns good
505 representations for multitask imitation. In *NeurIPS*, 2023.
506507 Zhe Chen, Jiannan Wu, Wenhui Wang, Weijie Su, Guo Chen, Sen Xing, Muyan Zhong, Qinglong
508 Zhang, Xizhou Zhu, Lewei Lu, et al. Internvl: Scaling up vision foundation models and aligning
509 for generic visual-linguistic tasks. In *Proceedings of the IEEE/CVF conference on computer vision*
510 and pattern recognition, pp. 24185–24198, 2024.511 Kanzhi Cheng, Qiushi Sun, Yougang Chu, Fangzhi Xu, Yantao Li, Jianbing Zhang, and Zhiyong Wu.
512 Seeclick: Harnessing GUI grounding for advanced visual GUI agents. In *ACL (1)*, pp. 9313–9332.
513 Association for Computational Linguistics, 2024.
514515 Gaole Dai, Shiqi Jiang, Ting Cao, Yuanchun Li, Yuqing Yang, Rui Tan, Mo Li, and Lili Qiu.
516 Advancing mobile gui agents: A verifier-driven approach to practical deployment. *arXiv preprint*
517 *arXiv:2503.15937*, 2025.518 Biplab Deka, Zifeng Huang, Chad Franzen, Joshua Hirschman, Daniel Afergan, Yang Li, Jeffrey
519 Nichols, and Ranjitha Kumar. Rico: A mobile app dataset for building data-driven design
520 applications. In *UIST*, pp. 845–854. ACM, 2017.
521522 Longxi Gao, Li Zhang, Shihe Wang, Shangguang Wang, Yuanchun Li, and Mengwei Xu. Mobile-
523 views: A large-scale mobile gui dataset. *arXiv preprint arXiv:2409.14337*, 2024.524 Boyu Gou, Ruohan Wang, Boyuan Zheng, Yanan Xie, Cheng Chang, Yiheng Shu, Huan Sun, and
525 Yu Su. Navigating the digital world as humans do: Universal visual grounding for gui agents.
526 *arXiv preprint arXiv:2410.05243*, 2024.527 Zhangxuan Gu, Zhengwen Zeng, Zhenyu Xu, Xingran Zhou, Shuheng Shen, Yunfei Liu, Beitong
528 Zhou, Changhua Meng, Tianyu Xia, Weizhi Chen, et al. Ui-venus technical report: Building
529 high-performance ui agents with rft. *arXiv preprint arXiv:2508.10833*, 2025.
530531 Daya Guo, Dejian Yang, Haowei Zhang, Junxiao Song, Ruoyu Zhang, Runxin Xu, Qihao Zhu,
532 Shirong Ma, Peiyi Wang, Xiao Bi, et al. Deepseek-r1: Incentivizing reasoning capability in llms
533 via reinforcement learning. *arXiv preprint arXiv:2501.12948*, 2025.534 Wenyi Hong, Weihan Wang, Qingsong Lv, Jiazheng Xu, Wenmeng Yu, Junhui Ji, Yan Wang, Zihan
535 Wang, Yuxiao Dong, Ming Ding, and Jie Tang. Cogagent: A visual language model for GUI agents.
536 In *CVPR*, pp. 14281–14290. IEEE, 2024.
537538 Nathan Lambert, Jacob Morrison, Valentina Pyatkin, Shengyi Huang, Hamish Ivison, Faeze Brahman,
539 Lester James V Miranda, Alisa Liu, Nouha Dziri, Shane Lyu, et al. T\ulu 3: Pushing frontiers in
open language model post-training. *arXiv preprint arXiv:2411.15124*, 2024.

540 Kaixin Li, Ziyang Meng, Hongzhan Lin, Ziyang Luo, Yuchen Tian, Jing Ma, Zhiyong Huang, and
 541 Tat-Seng Chua. Screenspot-pro: Gui grounding for professional high-resolution computer use.
 542 *arXiv preprint arXiv:2504.07981*, 2025a.

543

544 Kaixin Li, Meng Ziyang, Hongzhan Lin, Ziyang Luo, Yuchen Tian, Jing Ma, Zhiyong Huang, and
 545 Tat-Seng Chua. Screenspot-pro: GUI grounding for professional high-resolution computer use.
 546 In *Workshop on Reasoning and Planning for Large Language Models*, 2025b. URL <https://openreview.net/forum?id=XaKNDIAHas>.

547

548 Wei Li, William E. Bishop, Alice Li, Christopher Rawles, Folawiyo Campbell-Ajala, Divya Tyamagundlu, and Oriana Riva. On the effects of data scale on UI control agents. In *NeurIPS*,
 549 2024.

550

552 Kevin Qinghong Lin, Linjie Li, Difei Gao, Zhengyuan Yang, Shiwei Wu, Zechen Bai, Weixian Lei,
 553 Lijuan Wang, and Mike Zheng Shou. Showui: One vision-language-action model for gui visual
 554 agent. *arXiv preprint arXiv:2411.17465*, 2024.

555

556 Yuhang Liu, Pengxiang Li, Congkai Xie, Xavier Hu, Xiaotian Han, Shengyu Zhang, Hongxia Yang,
 557 and Fei Wu. Infigui-r1: Advancing multimodal gui agents from reactive actors to deliberative
 558 reasoners. *arXiv preprint arXiv:2504.14239*, 2025.

559

560 Quanfeng Lu, Wenqi Shao, Zitao Liu, Fanqing Meng, Boxuan Li, Botong Chen, Siyuan Huang,
 561 Kaipeng Zhang, Yu Qiao, and Ping Luo. Gui odyssey: A comprehensive dataset for cross-app gui
 562 navigation on mobile devices. *arXiv preprint arXiv:2406.08451*, 2024.

563

564 Zhengxi Lu, Yuxiang Chai, Yaxuan Guo, Xi Yin, Liang Liu, Hao Wang, Han Xiao, Shuai Ren, Guan-
 565 jing Xiong, and Hongsheng Li. Ui-r1: Enhancing action prediction of gui agents by reinforcement
 566 learning. *arXiv preprint arXiv:2503.21620*, 2025.

567

568 OpenAI. Gpt-4o system card. *arXiv preprint arXiv:2410.21276*, 2024.

569

570 Yujia Qin, Yining Ye, Junjie Fang, Haoming Wang, Shihao Liang, Shizuo Tian, Junda Zhang, Jiahao
 571 Li, Yunxin Li, Shijue Huang, et al. Uti-tars: Pioneering automated gui interaction with native
 572 agents. *arXiv preprint arXiv:2501.12326*, 2025.

573

574 Christopher Rawles, Alice Li, Daniel Rodriguez, Oriana Riva, and Timothy Lillicrap. An-
 575 droidinthewild: A large-scale dataset for android device control. *Advances in Neural Information
 576 Processing Systems*, 36:59708–59728, 2023.

577

578 Christopher Rawles, Sarah Clinckemaillie, Yifan Chang, Jonathan Waltz, Gabrielle Lau, Marybeth
 579 Fair, Alice Li, William Bishop, Wei Li, Folawiyo Campbell-Ajala, et al. Androidworld: A dynamic
 580 benchmarking environment for autonomous agents. *arXiv preprint arXiv:2405.14573*, 2024.

581

582 John Schulman, Filip Wolski, Prafulla Dhariwal, Alec Radford, and Oleg Klimov. Proximal policy
 583 optimization algorithms. *arXiv preprint arXiv:1707.06347*, 2017.

584

585 Zhihong Shao, Peiyi Wang, Qihao Zhu, Runxin Xu, Junxiao Song, Xiao Bi, Haowei Zhang,
 586 Mingchuan Zhang, YK Li, Y Wu, et al. Deepseekmath: Pushing the limits of mathematical
 587 reasoning in open language models. *arXiv preprint arXiv:2402.03300*, 2024.

588

589 Haozhan Shen, Peng Liu, Jingcheng Li, Chunxin Fang, Yibo Ma, Jiajia Liao, Qiaoli Shen, Zilun
 590 Zhang, Kangjia Zhao, Qianqian Zhang, et al. Vlm-r1: A stable and generalizable r1-style large
 591 vision-language model. *arXiv preprint arXiv:2504.07615*, 2025.

592

593 Jiaqi Tang, Yu Xia, Yi-Feng Wu, Yuwei Hu, Yuhui Chen, Qing-Guo Chen, Xiaogang Xu, Xiangyu Wu,
 594 Hao Lu, Yanqing Ma, et al. Lpo: Towards accurate gui agent interaction via location preference
 595 optimization. *arXiv preprint arXiv:2506.09373*, 2025.

596

597 Yang Tian, Sizhe Yang, Jia Zeng, Ping Wang, Dahua Lin, Hao Dong, and Jiangmiao Pang. Pre-
 598 dictive inverse dynamics models are scalable learners for robotic manipulation. *arXiv preprint
 599 arXiv:2412.15109*, 2024.

594 Weihuan Wang, Qingsong Lv, Wenmeng Yu, Wenyi Hong, Ji Qi, Yan Wang, Junhui Ji, Zhuoyi Yang,
 595 Lei Zhao, Xixuan Song, Jiazheng Xu, Keqin Chen, Bin Xu, Juanzi Li, Yuxiao Dong, Ming Ding,
 596 and Jie Tang. Cogvlm: Visual expert for pretrained language models. In *NeurIPS*, 2024.

597

598 Hao Wen, Yuanchun Li, Guohong Liu, Shanhui Zhao, Tao Yu, Toby Jia-Jun Li, Shiqi Jiang, Yunhao
 599 Liu, Yaqin Zhang, and Yunxin Liu. Autodroid: Llm-powered task automation in android. In
 600 *MobiCom*, pp. 543–557. ACM, 2024.

601 Qinzhuo Wu, Weikai Xu, Wei Liu, Tao Tan, Jianfeng Liu, Ang Li, Jian Luan, Bin Wang, and Shuo
 602 Shang. Mobilevlm: A vision-language model for better intra- and inter-ui understanding. In
 603 *EMNLP (Findings)*, pp. 10231–10251. Association for Computational Linguistics, 2024a.

604

605 Zhiyong Wu, Zhenyu Wu, Fangzhi Xu, Yian Wang, Qiushi Sun, Chengyou Jia, Kanzhi Cheng, Zichen
 606 Ding, Liheng Chen, Paul Pu Liang, et al. Os-atlas: A foundation action model for generalist gui
 607 agents. *arXiv preprint arXiv:2410.23218*, 2024b.

608 Xiaobo Xia and Run Luo. Gui-r1: A generalist r1-style vision-language action model for gui agents.
 609 *arXiv preprint arXiv:2504.10458*, 2025.

610

611 Xiaomi. Guievalkit: Open-source evaluation toolkit for gui agents. <https://github.com/xiaomi-research/guievalkit>, 2025a. Accessed: 2025-09-25.

612

613 LLM-Core-Team Xiaomi. Mimo-vl technical report. *arXiv preprint arXiv:2506.03569*, 2025b.

614

615 Yiheng Xu, Zekun Wang, Junli Wang, Dunjie Lu, Tianbao Xie, Amrita Saha, Doyen Sahoo, Tao Yu,
 616 and Caiming Xiong. Aguvis: Unified pure vision agents for autonomous gui interaction. *arXiv
 617 preprint arXiv:2412.04454*, 2024.

618 Yuhao Yang, Yue Wang, Dongxu Li, Ziyang Luo, Bei Chen, Chao Huang, and Junnan Li. Aria-ui:
 619 Visual grounding for gui instructions. *arXiv preprint arXiv:2412.16256*, 2024.

620

621 Samuel Zapolsky and Evan M. Drumwright. Inverse dynamics with rigid contact and friction. *Auton.
 622 Robots*, 41(4):831–863, 2017.

623

624 Li Zhang, Longxi Gao, and Mengwei Xu. Does chain-of-thought reasoning help mobile gui agent?
 625 an empirical study. *arXiv preprint arXiv:2503.16788*, 2025a.

626

627 Zhong Zhang, Yaxi Lu, Yikun Fu, Yupeng Huo, Shenzhi Yang, Yesai Wu, Han Si, Xin Cong, Haotian
 628 Chen, Yankai Lin, Jie Xie, Wei Zhou, Wang Xu, Yuanheng Zhang, Zhou Su, Zhongwu Zhai,
 629 Xiaoming Liu, Yudong Mei, Jianming Xu, Hongyan Tian, Chongyi Wang, Chi Chen, Yuan Yao,
 630 Zhiyuan Liu, and Maosong Sun. AgentCPM-GUI: Building mobile-use agents with reinforcement
 631 fine-tuning. *arXiv preprint arXiv:2506.01391*, 2025b.

632

633

634

635

636

637

638

639

640

641

642

643

644

645

646

647

648 A USE OF LARGE LANGUAGE MODELS (LLMs)
649650 We use LLMs for writing polishing and language refinement.
651652 B TRAINING HYPER-PARAMETERS
653654 The hyper-parameter details for GUI-Shift are provided in Table 4.
655656
657 Table 4: Hyper-parameter settings used for all GRPO training.
658

659 Hyper-parameter	659 Value
660 learning_rate	660 from 1e-6 to 0
661 temperature	661 0.9
662 num_generations	662 8
663 num_train_epochs	663 4
664 max_prompt_length	664 1024
665 max_completion_length	665 256
666 per_device_train_batch_size	666 2
667 gradient_accumulation_steps	667 8
668 ϵ (clipping parameter)	668 0.2
669 β (KL coefficient)	669 0.04

670
671
672
673
674
675
676
677
678
679
680
681
682
683
684
685
686
687
688
689
690
691
692
693
694
695
696
697
698
699
700
701

702 C TASK AUTOMATION RESULTS WITH AND WITHOUT DATA FILTERING

704 Table 5 and Table 6 report the performance of GUI-Shift on AndroidControl and GUI Odyssey
 705 benchmarks using 2K K -step GUI Transition samples, with and without data filtering. Without data
 706 filtering, as shown in Table 5, GUI-Shift trained with each k value outperforms the base models on
 707 most benchmarks. Specifically, for Qwen2.5-VL-7B, GUI-Shift delivers consistent improvements
 708 across all benchmarks; for the other three models, GUI-Shift also improves task automation in most
 709 cases, especially on AndroidControl. These results demonstrate that conditioning on the future state
 710 S_{t+k} consistently provides an effective supervision signal across different transition step sizes. We
 711 apply data filtering to InternVL3-8B, MimoVL-7B-SFT, and MimoVL-7B-RL. With data filtering,
 712 as shown in Table 6, model performance further improves in most settings, confirming that filtering
 713 enhances data quality and strengthens VLM optimization.

714
 715 Table 5: Performance on task automation benchmarks: AndroidControl and GUI Odyssey. Models
 716 are fine-tuned with 2K k -step UI Transition samples for each $k \in \{1, 2, 3, 4\}$, **without model-specific**
 717 **data filtering**. The target states S_{t+k} with different k values provide effective visual instructions for
 718 GUI agent training. TM: type match; GR: grounding accuracy for clicks; EM: exact match.

720 Model	721 AndroidControl-Low			721 AndroidControl-High			721 GUI Odyssey		
	722 TM	722 GR	722 EM	723 TM	723 GR	723 EM	724 TM	724 GR	724 EM
722 Qwen2.5-VL-7B	94.9	90.9	83.8	72.9	66.6	59.2	59.8	47.5	44.9
723 GUI-Shift-Qwen ($k = 1$)	98.0 \uparrow 3.1	94.0 \uparrow 3.1	90.6 \uparrow 6.8	85.9 \uparrow 13.0	77.5 \uparrow 10.9	70.4 \uparrow 11.2	78.5 \uparrow 18.7	67.2 \uparrow 19.7	54.8 \uparrow 9.9
724 GUI-Shift-Qwen ($k = 2$)	98.0 \uparrow 3.1	93.7 \uparrow 2.8	90.0 \uparrow 6.2	85.9 \uparrow 13.0	76.9 \uparrow 10.3	70.8 \uparrow 11.6	79.4 \uparrow 19.6	68.6 \uparrow 21.1	55.7 \uparrow 10.8
725 GUI-Shift-Qwen ($k = 3$)	97.9 \uparrow 3.0	93.6 \uparrow 2.7	91.5 \uparrow 7.7	85.3 \uparrow 12.4	77.7 \uparrow 11.1	70.0 \uparrow 10.8	77.1 \uparrow 17.3	67.6 \uparrow 20.1	53.8 \uparrow 8.9
726 GUI-Shift-Qwen ($k = 4$)	97.8 \uparrow 2.9	92.8 \uparrow 1.9	91.0 \uparrow 7.2	84.8 \uparrow 11.9	77.1 \uparrow 10.5	69.6 \uparrow 10.4	76.0 \uparrow 16.2	65.7 \uparrow 18.2	53.1 \uparrow 8.2
727 InternVL3-8B	97.8	92.4	90.0	71.5	54.6	49.8	48.8	20.2	20.3
728 GUI-Shift-Intern ($k = 1$)	98.1 \uparrow 0.3	92.8 \uparrow 0.4	89.6 \downarrow 0.4	73.1 \uparrow 1.6	56.0 \uparrow 1.4	52.5 \uparrow 2.7	42.9 \downarrow 5.9	17.6 \downarrow 2.6	17.9 \downarrow 2.4
729 GUI-Shift-Intern ($k = 2$)	97.6 \downarrow 0.2	92.9 \uparrow 0.5	87.9 \downarrow 2.1	76.3 \uparrow 4.8	59.8 \uparrow 5.2	54.3 \uparrow 4.5	59.4 \uparrow 10.6	24.4 \uparrow 4.2	23.1 \uparrow 2.8
730 GUI-Shift-Intern ($k = 3$)	97.5 \downarrow 0.3	92.6 \uparrow 0.2	89.3 \downarrow 0.7	78.6 \uparrow 7.1	61.7 \uparrow 7.1	58.2 \uparrow 8.4	51.4 \uparrow 2.6	21.4 \uparrow 1.2	21.4 \uparrow 1.1
731 GUI-Shift-Intern ($k = 4$)	97.3 \downarrow 0.5	92.9 \uparrow 0.5	88.0 \downarrow 2.0	78.5 \uparrow 7.0	64.3 \uparrow 9.7	56.6 \uparrow 6.8	59.6 \uparrow 10.8	25.9 \uparrow 5.7	23.3 \uparrow 3.0
732 Mimo-VL-7B-SFT	90.8	93.5	85.7	75.2	75.7	63.1	86.9	66.3	62.0
733 GUI-Shift-Mimo-SFT ($k = 1$)	98.6 \uparrow 7.8	93.8 \uparrow 0.3	92.0 \uparrow 6.3	86.8 \uparrow 11.6	74.3 \downarrow 1.4	71.7 \uparrow 8.6	85.4 \downarrow 1.5	67.1 \uparrow 0.8	61.3 \downarrow 0.7
734 GUI-Shift-Mimo-SFT ($k = 2$)	98.5 \uparrow 7.7	92.7 \downarrow 0.8	90.0 \uparrow 4.3	87.0 \uparrow 11.8	73.9 \downarrow 1.8	70.3 \uparrow 7.2	85.0 \downarrow 1.9	66.0 \downarrow 0.3	59.5 \downarrow 2.5
735 GUI-Shift-Mimo-SFT ($k = 3$)	98.2 \uparrow 7.4	92.5 \downarrow 1.0	88.4 \uparrow 2.7	85.5 \uparrow 10.3	72.2 \downarrow 3.5	68.1 \uparrow 5.0	86.0 \downarrow 0.9	65.4 \downarrow 0.9	58.5 \downarrow 3.5
736 GUI-Shift-Mimo-SFT ($k = 4$)	98.3 \uparrow 7.5	93.0 \downarrow 0.5	92.2 \uparrow 6.5	86.9 \uparrow 11.7	73.4 \downarrow 2.3	72.4 \uparrow 9.3	85.9 \downarrow 1.0	67.7 \uparrow 1.4	60.1 \downarrow 1.9
737 Mimo-VL-7B-RL	91.8	94.5	87.2	76.5	77.5	64.6	87.2	67.9	63.1
738 GUI-Shift-Mimo-RL ($k = 1$)	98.7 \uparrow 6.9	94.7 \uparrow 0.2	92.5 \uparrow 5.3	86.7 \uparrow 10.2	77.0 \downarrow 0.5	70.8 \uparrow 6.2	85.0 \downarrow 2.2	67.8 \downarrow 0.1	59.1 \downarrow 4.0
739 GUI-Shift-Mimo-RL ($k = 2$)	98.7 \uparrow 6.9	93.3 \downarrow 1.2	88.2 \uparrow 1.0	86.1 \uparrow 9.6	72.7 \downarrow 4.8	69.0 \uparrow 4.4	85.3 \downarrow 1.9	66.2 \downarrow 1.7	59.4 \downarrow 3.7
740 GUI-Shift-Mimo-RL ($k = 3$)	98.0 \uparrow 6.2	93.8 \downarrow 0.7	89.1 \uparrow 1.9	85.8 \uparrow 9.3	73.6 \downarrow 3.9	68.8 \uparrow 4.2	85.9 \downarrow 1.3	66.0 \downarrow 1.9	58.8 \downarrow 4.3
741 GUI-Shift-Mimo-RL ($k = 4$)	98.5 \uparrow 6.7	93.0 \downarrow 1.5	89.5 \uparrow 2.3	86.6 \uparrow 10.1	73.0 \downarrow 4.5	70.1 \uparrow 5.5	85.3 \downarrow 1.9	66.1 \downarrow 1.8	57.5 \downarrow 5.6

742
 743
 744
 745
 746
 747
 748
 749
 750
 751
 752
 753
 754
 755

Table 6: Performance on task automation benchmarks: AndroidControl and GUI Odyssey. Compared to training without data filtering, applying filtering yields greater improvements in most cases. TM: type match; GR: grounding accuracy for clicks; EM: exact match.

Model	Android Control-Low			Android Control-High			GUI Odyssey		
	TM	GR	EM	TM	GR	EM	TM	GR	EM
InternVL3-8B	97.8	92.4	90.0	71.5	54.6	49.8	48.8	20.2	20.3
GUI-Shift-Intern ($k = 1$)	96.2 $\downarrow 1.6$	92.6 $\uparrow 0.2$	87.0 $\downarrow 3.0$	78.6 $\uparrow 7.1$	63.2 $\uparrow 8.6$	55.1 $\uparrow 5.3$	51.6 $\uparrow 2.8$	24.5 $\uparrow 4.3$	22.1 $\uparrow 1.8$
GUI-Shift-Intern ($k = 2$)	97.2 $\downarrow 0.6$	92.3 $\downarrow 0.1$	86.4 $\downarrow 3.6$	79.4 $\uparrow 7.9$	63.3 $\uparrow 8.7$	55.9 $\uparrow 6.1$	51.9 $\uparrow 3.1$	24.4 $\uparrow 4.2$	23.9 $\uparrow 3.6$
GUI-Shift-Intern ($k = 3$)	96.3 $\downarrow 1.5$	92.7 $\uparrow 0.3$	87.7 $\downarrow 2.3$	79.9 $\uparrow 8.4$	65.5 $\uparrow 10.9$	57.6 $\uparrow 7.8$	59.5 $\uparrow 10.7$	27.2 $\uparrow 7.0$	24.8 $\uparrow 4.5$
GUI-Shift-Intern ($k = 4$)	96.2 $\downarrow 1.6$	92.8 $\uparrow 0.4$	87.7 $\downarrow 2.3$	81.0 $\uparrow 9.5$	67.8 $\uparrow 13.2$	59.9 $\uparrow 10.1$	57.0 $\uparrow 8.2$	27.4 $\uparrow 7.2$	25.7 $\uparrow 5.4$
Mimo-VL-7B-SFT	90.8	93.5	85.7	75.2	75.7	63.1	86.9	66.3	62.0
GUI-Shift-Mimo-SFT ($k = 1$)	97.8 $\uparrow 7.0$	93.8 $\uparrow 0.3$	92.2 $\uparrow 6.5$	84.6 $\uparrow 9.4$	75.7 $\uparrow 0.0$	70.2 $\uparrow 7.1$	81.8 $\downarrow 5.1$	64.3 $\downarrow 2.0$	56.2 $\downarrow 5.8$
GUI-Shift-Mimo-SFT ($k = 2$)	98.6 $\uparrow 7.8$	93.3 $\downarrow 0.2$	92.9 $\uparrow 7.2$	86.4 $\uparrow 11.2$	75.8 $\uparrow 0.1$	72.0 $\uparrow 8.9$	85.2 $\downarrow 1.7$	66.6 $\uparrow 0.3$	60.3 $\downarrow 1.7$
GUI-Shift-Mimo-SFT ($k = 3$)	98.6 $\uparrow 7.8$	94.0 $\uparrow 0.5$	93.2 $\uparrow 7.5$	87.2 $\uparrow 12.0$	75.6 $\downarrow 0.1$	73.4 $\uparrow 10.3$	86.1 $\downarrow 0.8$	66.3 $\uparrow 0.0$	60.7 $\downarrow 1.3$
GUI-Shift-Mimo-SFT ($k = 4$)	98.6 $\uparrow 7.8$	93.5 $\uparrow 0.0$	92.7 $\uparrow 7.0$	85.8 $\uparrow 10.6$	73.9 $\downarrow 1.8$	71.6 $\uparrow 8.5$	85.9 $\downarrow 1.0$	67.5 $\uparrow 1.2$	60.9 $\downarrow 1.1$
Mimo-VL-7B-RL	91.8	94.5	87.2	76.5	77.5	64.6	87.2	67.9	63.1
GUI-Shift-Mimo-RL ($k = 1$)	98.9 $\uparrow 7.1$	94.3 $\downarrow 0.2$	93.2 $\uparrow 6.0$	86.9 $\uparrow 10.4$	75.9 $\downarrow 1.6$	71.7 $\uparrow 7.1$	84.8 $\downarrow 2.4$	67.5 $\downarrow 0.4$	59.5 $\downarrow 3.6$
GUI-Shift-Mimo-RL ($k = 2$)	97.7 $\uparrow 5.9$	93.7 $\downarrow 0.8$	91.3 $\uparrow 4.1$	87.6 $\uparrow 11.1$	75.9 $\downarrow 1.6$	71.6 $\uparrow 7.0$	84.9 $\downarrow 2.3$	65.4 $\downarrow 2.5$	58.9 $\downarrow 4.2$
GUI-Shift-Mimo-RL ($k = 3$)	97.3 $\uparrow 5.5$	93.9 $\downarrow 0.6$	91.1 $\uparrow 3.9$	87.1 $\uparrow 10.6$	77.3 $\downarrow 0.2$	71.7 $\uparrow 7.1$	84.9 $\downarrow 2.3$	67.6 $\downarrow 0.3$	59.7 $\downarrow 3.4$
GUI-Shift-Mimo-RL ($k = 4$)	96.8 $\uparrow 5.0$	94.2 $\downarrow 0.3$	90.9 $\uparrow 3.7$	87.0 $\uparrow 10.5$	77.0 $\downarrow 0.5$	72.1 $\uparrow 7.5$	84.7 $\downarrow 2.5$	68.3 $\uparrow 0.4$	59.9 $\downarrow 3.2$

810 D GROUNDING RESULTS WITH AND WITHOUT DATA FILTERING 811

812 We report the accuracy of GUI-Shift on two GUI grounding benchmarks: ScreenSpot-v2 and
813 ScreenSpot-Pro, under both filtered and unfiltered settings.

814 For ScreenSpot-v2 (Table 7), all models except GUI-Shift-Intern achieve consistent improvements
815 over their respective baselines without data filtering. With data filtering (Table 8), GUI-Shift-Intern
816 models also surpass their baselines, indicating the benefit of filtering.

817 For ScreenSpot-Pro (Table 9), all GUI-Shift-Qwen models improve without data filtering, while
818 other models exhibit mixed results across different k . We attribute the performance drop to the
819 high-resolution desktop screenshots in ScreenSpot-Pro, which are not present in our training data.
820 With data filtering (Table 10), GUI-Shift-Mimo-RL achieves consistent gains for all k .

821 Overall, GUI-Shift demonstrates strong generalization on GUI grounding, with performance gains in
822 most cases, especially when data filtering is applied.

823
824
825 Table 7: Performance on GUI grounding benchmark: ScreenSpot-v2. Models are fine-tuned with 2K
826 k -step UI Transition samples for each $k \in \{1, 2, 3, 4\}$, **without model-specific data filtering**.

827 828 829 830 831 832 833 834 835 836 837 838 839 840 841 842 843 844 845 846 847 848 849 850 851 852 853 854 855 856 857 858 859 860 861 862 863 Model	830 831 832 833 834 835 836 837 838 839 840 841 842 843 844 845 846 847 848 849 850 851 852 853 854 855 856 857 858 859 860 861 862 863 Mobile			830 831 832 833 834 835 836 837 838 839 840 841 842 843 844 845 846 847 848 849 850 851 852 853 854 855 856 857 858 859 860 861 862 863 Desktop			830 831 832 833 834 835 836 837 838 839 840 841 842 843 844 845 846 847 848 849 850 851 852 853 854 855 856 857 858 859 860 861 862 863 Web			830 831 832 833 834 835 836 837 838 839 840 841 842 843 844 845 846 847 848 849 850 851 852 853 854 855 856 857 858 859 860 861 862 863 Avg.
	830 831 832 833 834 835 836 837 838 839 840 841 842 843 844 845 846 847 848 849 850 851 852 853 854 855 856 857 858 859 860 861 862 863 Text	830 831 832 833 834 835 836 837 838 839 840 841 842 843 844 845 846 847 848 849 850 851 852 853 854 855 856 857 858 859 860 861 862 863 Icon	830 831 832 833 834 835 836 837 838 839 840 841 842 843 844 845 846 847 848 849 850 851 852 853 854 855 856 857 858 859 860 861 862 863 Avg.							
Qwen2.5-VL-7B	98.3	86.3	93.2	88.7	67.1	79.6	92.7	81.8	87.6	87.7
GUI-Shift-Qwen ($k = 1$)	98.6	87.7	94.0	88.1	71.4	81.1	92.7	81.8	87.6	88.4 ^{↑0.7}
GUI-Shift-Qwen ($k = 2$)	98.6	89.1	94.6	87.6	73.6	81.7	92.3	80.8	87.0	88.6 ^{↑0.9}
GUI-Shift-Qwen ($k = 3$)	99.0	88.6	94.6	86.1	72.9	80.5	92.3	80.8	87.0	88.3 ^{↑0.6}
GUI-Shift-Qwen ($k = 4$)	98.6	89.6	94.8	86.1	75.0	81.4	92.7	82.8	88.1	89.0 ^{↑1.3}
InternVL3-8B	93.4	81.5	88.4	80.4	52.1	68.6	91	73.4	82.8	81.3
GUI-Shift-Intern ($k = 1$)	94.1	81.5	88.8	77.3	52.1	66.8	91.5	73.4	83.1	81.1 ^{↓0.2}
GUI-Shift-Intern ($k = 2$)	93.8	80.6	88.2	80.4	52.1	68.6	91.5	72.4	82.6	81.1 ^{↓0.2}
GUI-Shift-Intern ($k = 3$)	94.8	80.1	88.6	78.9	47.1	65.6	90.6	71.4	81.7	80.2 ^{↓0.9}
GUI-Shift-Intern ($k = 4$)	94.1	82.0	89.0	79.4	54.3	68.9	91.9	71.9	82.6	81.5 ^{↑0.2}
Mimo-VL-7B-SFT	96.6	84.4	91.4	92.8	80.0	87.4	88.9	76.8	83.3	87.6
GUI-Shift-Mimo-SFT ($k = 1$)	97.2	86.3	92.6	91.8	79.3	86.5	90.6	74.9	83.3	87.8 ^{↑0.2}
GUI-Shift-Mimo-SFT ($k = 2$)	95.9	84.4	91.0	92.8	82.9	88.6	91.9	75.9	84.4	88.1 ^{↑0.5}
GUI-Shift-Mimo-SFT ($k = 3$)	96.6	86.3	92.2	91.8	82.9	88.0	90.6	77.3	84.4	88.4 ^{↑0.8}
GUI-Shift-Mimo-SFT ($k = 4$)	96.9	87.2	92.8	91.8	84.3	88.6	89.7	80.3	85.4	89.2 ^{↑1.6}
Mimo-VL-7B-RL	98.3	86.3	93.2	90.2	80.7	86.2	92.7	75.4	84.7	88.4
GUI-Shift-Mimo-RL ($k = 1$)	99.3	88.2	94.6	91.8	80.7	87.1	90.2	75.4	83.3	88.8 ^{↑0.4}
GUI-Shift-Mimo-RL ($k = 2$)	97.9	87.2	93.4	91.8	81.4	87.4	91	74.4	83.3	88.4 ^{↑0.0}
GUI-Shift-Mimo-RL ($k = 3$)	98.3	87.2	93.6	91.8	83.6	88.3	91	76.4	84.2	89.0 ^{↑0.6}
GUI-Shift-Mimo-RL ($k = 4$)	99.3	87.7	94.4	91.8	81.4	87.4	90.6	75.4	83.5	88.8 ^{↑0.4}

864
865
866867 Table 8: Performance on GUI grounding benchmark: ScreenSpot-v2. **Model-specific data filtering**
868 **is applied** to InternVL3-8B, MimoVL-7B-SFT, and MimoVL-7B-RL. For each model, we select 2K
869 k -step UI Transition samples for each $k \in \{1, 2, 3, 4\}$ from a pool of candidates.

870

Model	Mobile			Desktop			Web			Avg.
	Text	Icon	Avg.	Text	Icon	Avg.	Text	Icon	Avg.	
InternVL3-8B	93.4	81.5	88.4	80.4	52.1	68.6	91.0	73.4	82.8	81.3
GUI-Shift-Intern ($k = 1$)	93.8	83.4	89.4	80.4	51.4	68.3	91.0	73.4	82.8	81.6 ^{↑0.3}
GUI-Shift-Intern ($k = 2$)	94.5	82	89.2	78.9	51.4	67.4	91.9	72.4	82.8	81.3 ^{↑0.0}
GUI-Shift-Intern ($k = 3$)	94.5	83.4	89.8	79.4	50.7	67.4	91.9	73.4	83.3	81.7 ^{↑0.4}
GUI-Shift-Intern ($k = 4$)	93.4	83.4	89.2	77.8	54.3	68.0	91.5	73.9	83.3	81.6 ^{↑0.3}
Mimo-VL-7B-SFT	96.6	84.4	91.4	92.8	80.0	87.4	88.9	76.8	83.3	87.6
GUI-Shift-Mimo-SFT ($k = 1$)	98.3	87.7	93.8	92.3	82.1	88.0	94.0	79.8	87.4	90.1 ^{↑2.5}
GUI-Shift-Mimo-SFT ($k = 2$)	98.6	87.7	94.0	93.3	83.6	89.2	92.7	79.8	86.7	90.3 ^{↑2.7}
GUI-Shift-Mimo-SFT ($k = 3$)	96.6	85.3	91.8	91.8	81.4	87.4	89.3	80.3	85.1	88.4 ^{↑0.8}
GUI-Shift-Mimo-SFT ($k = 4$)	97.6	83.9	91.8	92.3	82.9	88.3	91.5	79.3	85.8	88.8 ^{↑1.2}
Mimo-VL-7B-RL	98.3	86.3	93.2	90.2	80.7	86.2	92.7	75.4	84.7	88.4
GUI-Shift-Mimo-RL ($k = 1$)	99.0	87.7	94.2	91.2	83.6	88.0	89.7	72.9	81.9	88.4 ^{↑0.0}
GUI-Shift-Mimo-RL ($k = 2$)	97.9	86.7	93.2	90.7	80.7	86.5	91.0	75.4	83.8	88.2 ^{↓0.2}
GUI-Shift-Mimo-RL ($k = 3$)	99.0	87.2	94.0	91.8	80.7	87.1	91.0	76.8	84.4	88.9 ^{↑0.5}
GUI-Shift-Mimo-RL ($k = 4$)	98.6	85.3	93	91.8	81.4	87.4	91.9	77.3	85.1	88.8 ^{↑0.4}

887

888

889

890

891

892

893 Table 9: Performance on GUI grounding benchmark: ScreenSpot-Pro. Models are fine-tuned with
894 2K k -step UI Transition samples for each $k \in \{1, 2, 3, 4\}$, **without model-specific data filtering**.

895

Model	CAD		Dev		Creative		Scientific		Office		OS		Avg.
	Text	Icon	Text	Icon	Text	Icon	Text	Icon	Text	Icon	Text	Icon	
Qwen2.5-VL-7B	16.2	1.6	44.2	2.1	36.9	7.7	47.9	8.2	53.7	18.9	36.4	7.9	26.4
GUI-Shift-Qwen ($k = 1$)	16.2	4.7	52.6	9.0	27.3	7.0	52.1	5.5	49.7	17.0	38.3	13.5	26.8 ^{↑0.4}
GUI-Shift-Qwen ($k = 2$)	16.8	3.1	52.6	10.3	29.3	8.4	52.1	4.5	50.8	17.0	35.5	13.5	27.2 ^{↑0.8}
GUI-Shift-Qwen ($k = 3$)	15.7	3.1	52.6	9.7	30.3	7.0	50.7	5.5	48.0	15.1	35.5	12.4	26.5 ^{↑0.1}
GUI-Shift-Qwen ($k = 4$)	17.3	3.1	51.9	9.7	30.3	7.0	54.2	5.5	49.7	17.0	33.6	12.4	27.1 ^{↑0.7}
InternVL3-8B	8.6	4.7	27.3	4.1	27.3	0.7	24.3	4.5	32.2	3.8	11.2	3.4	15.0
GUI-Shift-Intern ($k = 1$)	10.2	1.6	27.3	4.8	26.8	0.7	23.6	3.6	33.9	7.5	15.0	2.2	15.4 ^{↑0.4}
GUI-Shift-Intern ($k = 2$)	7.6	3.1	27.3	3.4	28.3	0.7	21.5	4.5	33.3	7.5	12.1	2.2	14.9 ^{↓0.1}
GUI-Shift-Intern ($k = 3$)	9.6	3.1	23.4	5.5	26.3	0.7	20.1	1.8	29.9	3.8	11.2	1.1	13.7 ^{↓1.3}
GUI-Shift-Intern ($k = 4$)	9.1	4.7	24.0	4.1	28.8	0.7	21.5	3.6	31.1	3.8	13.1	1.1	14.5 ^{↓0.5}
Mimo-VL-7B-SFT	47.2	23.4	48.7	9.0	48.0	13.3	70.8	27.3	64.4	39.6	36.4	15.7	39.8
GUI-Shift-Mimo-SFT ($k = 1$)	49.7	15.6	46.8	13.8	49.0	16.1	74.3	25.5	65.0	37.7	40.2	15.7	40.9 ^{↑1.1}
GUI-Shift-Mimo-SFT ($k = 2$)	48.7	20.3	50.6	11.7	48.5	14.0	72.9	26.4	63.3	41.5	36.4	16.9	40.6 ^{↑0.8}
GUI-Shift-Mimo-SFT ($k = 3$)	45.7	18.8	48.1	12.4	45.5	12.6	70.1	28.2	65.5	39.6	35.5	19.1	39.6 ^{↓0.2}
GUI-Shift-Mimo-SFT ($k = 4$)	45.7	18.8	51.3	12.4	46.5	12.6	71.5	28.2	62.7	41.5	37.4	16.9	39.9 ^{↑0.1}
Mimo-VL-7B-RL	48.2	14.1	46.8	11.0	47.0	14.0	71.5	27.3	66.7	39.6	39.3	19.1	40.2
GUI-Shift-Mimo-RL ($k = 1$)	48.7	15.6	46.1	13.8	51.0	13.3	72.2	30.0	66.7	43.4	42.1	21.3	41.7 ^{↑1.5}
GUI-Shift-Mimo-RL ($k = 2$)	46.7	14.1	47.4	13.8	49.0	12.6	70.1	27.3	65.5	39.6	41.1	21.3	40.5 ^{↑0.3}
GUI-Shift-Mimo-RL ($k = 3$)	49.7	12.5	47.4	11.0	47.0	11.2	70.8	26.4	65.5	45.3	35.5	20.2	39.9 ^{↓0.3}
GUI-Shift-Mimo-RL ($k = 4$)	46.7	14.1	46.1	13.8	47.0	14.7	69.4	27.3	64.4	41.5	36.4	21.3	39.8 ^{↓0.4}

916

917

918

919
920
921
922
Table 10: Performance on GUI grounding benchmark: ScreenSpot-Pro. **Model-specific data**
923
filtering is applied to InternVL3-8B, MimoVL-7B-SFT, and MimoVL-7B-RL. For each model, we
924
select 2K k -step UI Transition samples for each $k \in \{1, 2, 3, 4\}$ from a pool of candidates.

Model	CAD		Dev		Creative		Scientific		Office		OS		Avg.
	Text	Icon	Text	Icon	Text	Icon	Text	Icon	Text	Icon	Text	Icon	
InternVL3-8B	8.6	4.7	27.3	4.1	27.3	0.7	24.3	4.5	32.2	3.8	11.2	3.4	15.0
GUI-Shift-Intern ($k = 1$)	11.2	3.1	26.6	5.5	28.8	0.7	20.1	4.5	33.9	7.5	13.1	1.1	15.4 $\uparrow 0.4$
GUI-Shift-Intern ($k = 2$)	8.1	1.6	26.0	4.1	26.3	0.7	25.7	1.8	31.1	5.7	14.0	1.1	14.5 $\downarrow 0.5$
GUI-Shift-Intern ($k = 3$)	8.6	1.6	27.3	4.1	25.3	0.7	21.5	1.8	33.3	5.7	14.0	1.1	14.4 $\downarrow 0.6$
GUI-Shift-Intern ($k = 4$)	8.1	1.6	27.9	4.8	26.8	0.0	22.9	2.7	32.8	3.8	10.3	2.2	14.5 $\downarrow 0.5$
Mimo-VL-7B-SFT	47.2	23.4	48.7	9.0	48.0	13.3	70.8	27.3	64.4	39.6	36.4	15.7	39.8
GUI-Shift-Mimo-SFT ($k = 1$)	49.2	14.1	50.0	9.0	48.0	11.9	73.6	29.1	54.3	43.4	38.3	15.7	40.7 $\uparrow 0.9$
GUI-Shift-Mimo-SFT ($k = 2$)	46.2	17.2	46.8	11.0	47.5	10.5	74.3	30.9	65.5	43.4	35.5	16.9	40.0 $\uparrow 0.2$
GUI-Shift-Mimo-SFT ($k = 3$)	50.8	15.6	47.4	13.8	47.0	12.6	69.4	24.5	65.0	41.5	38.3	19.1	40.2 $\uparrow 0.4$
GUI-Shift-Mimo-SFT ($k = 4$)	44.2	18.8	53.9	11.0	43.9	11.2	72.2	26.4	62.1	47.2	40.2	12.4	39.4 $\downarrow 0.4$
Mimo-VL-7B-RL	48.2	14.1	46.8	11.0	47.0	14.0	71.5	27.3	66.7	39.6	39.3	19.1	40.2
GUI-Shift-Mimo-RL ($k = 1$)	48.7	14.1	51.9	13.1	50.0	15.4	70.8	28.2	67.2	39.6	37.4	21.3	41.6 $\uparrow 1.4$
GUI-Shift-Mimo-RL ($k = 2$)	47.2	18.8	47.4	14.5	49.0	15.4	72.2	29.1	66.1	43.4	39.3	19.1	41.3 $\uparrow 0.9$
GUI-Shift-Mimo-RL ($k = 3$)	45.7	17.2	46.1	11.7	49.5	14.0	70.8	29.1	66.1	39.6	37.4	21.3	40.4 $\uparrow 0.2$
GUI-Shift-Mimo-RL ($k = 4$)	47.7	18.8	48.1	13.8	52.5	12.6	72.2	28.2	67.2	45.3	40.2	20.2	41.8 $\uparrow 1.6$

939

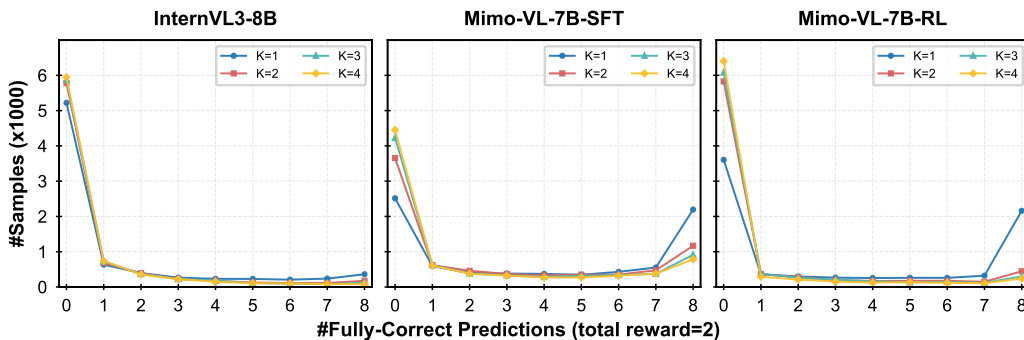
940

941

E REWARD DISTRIBUTION OF MODEL-SPECIFIC DATA FILTERING

942

943 To examine the relationship between the K value, task difficulty, and model capability, we analyze
944 the reward distributions obtained during the data filtering stage. Our analysis is based on 7,783 shared
945 samples. For fair comparison, we use exactly the same samples for each K across all models, and
946 the current state $S(t)$ and ground-truth actions remain identical across different K values. Figure E
947 presents the reward distributions for each model across different K values.



948
949
950
951
952
953
954
955
956
957
958
959
Figure 4: Comparison of reward distributions during model-specific data filtering. The x-axis
960 represents the number of fully-correct predictions, where $x = 0$ indicates all 8 rollouts are incorrect
961 and $x = 8$ indicates all 8 rollouts are correct. The y-axis reports how many K-step GUI Transition
962 samples fall into each fully-correct count.

963

964

We provide detailed analysis from two perspectives:

965

- **From the perspective of K .** (1) At $x = 0$, where all 8 rollouts are incorrect, the sample counts follow $K = 4 > 3 > 2 > 1$, indicating that larger K values correspond to higher difficulty. (2) At $x = 8$, where all 8 predictions are correct, the trend reverses to $K = 1 > 2 > 3 > 4$, showing that smaller K values are easier for the models.

966

967

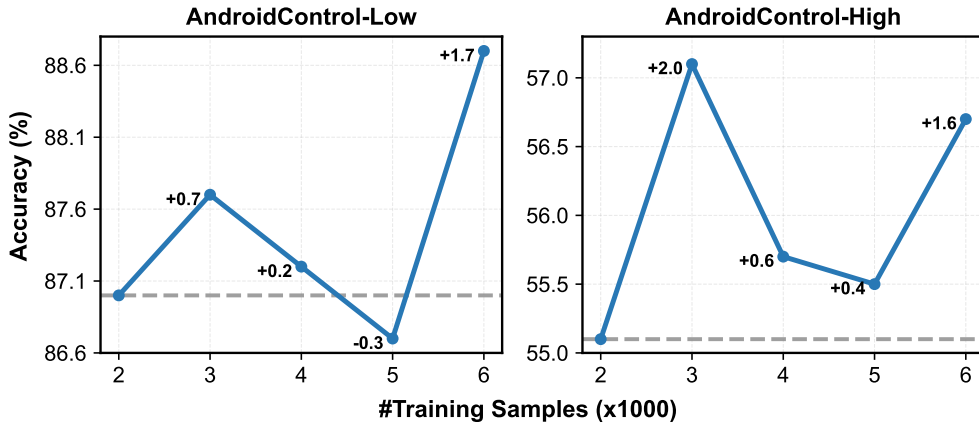
- **From the perspective of model capability.** As shown in Table 1 and Table 2, Mimo-VL-7B-SFT and Mimo-VL-7B-RL perform better than InternVL3-8B on four GUI-related benchmarks. We may

972 reasonably consider the Mimo models to have stronger GUI capability. A similar pattern appears in
 973 Figure E, both Mimo models have noticeably more samples at $x = 8$ than InternVL3-8B, suggesting
 974 that models with stronger GUI capability perform better on the K-step GUI Transition task.
 975

976 Overall, these findings reflects that the K-step GUI Transition task becomes more challenging as
 977 K increases, and that models with stronger GUI capability achieve better performance on this task,
 978 which aligns with intuition.

979 F INTERNVL3-8B PERFORMANCE SCALING WITH TRAINING DATA SIZE

980 To investigate how training data size affects GUI-Shift performance, we scale the training set from
 981 2K to 6K samples using K -step GUI Transition data ($K = 1$). Figure F illustrates the results on
 982 AndroidControl-Low and AndroidControl-High.
 983



1000 Figure 5: Performance on AndroidControl with InternVL3-8B trained on 1-step GUI Transition data.
 1001 Training samples are scaled from 2K to 6K. Accuracy exhibits an overall upward trend with only
 1002 minor fluctuations.
 1003

1004 Specifically, relative to the 2K setting, GUI-Shift-Intern shows an additional gain of 1.7% when
 1005 trained with 6K samples on AndroidControl-Low, and a further 2.0% improvement when trained with
 1006 3K samples on AndroidControl-High. In general, we observe an overall upward trend in accuracy as
 1007 the data size increases, with only small fluctuations across different scales.
 1008